

Calcium carbonate decomposition

Isabel Galan · Fredrik P. Glasser · Carmen Andrade

CEEC-TAC1 Conference Special Issue
© Akadémiai Kiadó, Budapest, Hungary 2012

Abstract Calcium carbonate decomposes under well-defined conditions giving CaO (solid) and CO₂ (gas). The process kinetics are known to be strongly influenced by the CO₂ partial pressure and temperature. In dynamic conditions, as in thermogravimetric analysis (TG) and differential thermal analysis (DTA), kinetics influence the observed heat effect and mass losses, as was shown in semi-static studies by Hyatt et al. (J Am Ceram Soc 41:70–74, 1). However, differing DTA and TG curve shapes are reported in the literature even under supposedly comparable conditions. The differences are attributed in part to the design of the equipment and in part to differing crystalline states of the precursor calcium carbonate. To resolve these uncertainties, the TG has been performed at different heating rates and at different but controlled partial pressures of CO₂. The results are reported and critically evaluated in the light of the data obtained, and the kinetic parameters as reported by Hyatt et al. (J Am Ceram Soc 41:70–74, 1) are re-evaluated.

Keywords Calcium carbonate · TG · Equilibrium · Kinetics

Introduction

Thermogravimetric analysis (TG) and differential thermal analysis (DTA) are widely used techniques in the field of

cement chemistry and are of particular interest for studying the carbonation of hydrated cement pastes [2–9]. During carbonation, the hydrated cement phases react with atmospheric CO₂ giving rise to the formation of calcium carbonate. For this reason, the amount of calcium carbonate present in a sample can be used as an indicator to evaluate severity of carbonation and its possible consequences, for example, in affecting corrosion of embedded steel reinforcement. To calculate the amount of CaCO₃, it is necessary correctly to delineate the temperature range in which decomposition takes place, identifying and correcting for possible couplings with other transformations involving mass changes.

Calcium carbonate decomposes to give CaO (solid) and CO₂ (gas). The process, as measured by TG, is influenced by intrinsic and extrinsic factors. Intrinsic factors include chemical purity and defect content of the sample, its surface area, crystallite size, morphology, etc. Extrinsic factors include sample packing, gas interchange between furnace atmosphere and the sample in the course of the test, severity of the thermal gradient developed in the sample as decomposition gets under way, etc. In dynamic conditions, as in TG and DTA, kinetics and equilibrium, i.e., CO₂ partial pressure and temperature, control the observed heat effect and mass losses, as was shown in semi-static studies by Hyatt et al. [1] using 0.1 × 1 × 1.5 cm crystals. Since then, many related studies have been published [10–28]. However, differing shapes are reported in the literature for DTA and TG curves, especially in the cement chemistry field. The differences are due at least in part to the choice of equipment and conditions (atmosphere, heating rate, etc.). But it is also reported that the differences arise in part from different crystalline states of the precursor calcium carbonate.

The objective of this research was to study the influence of the CO₂ partial pressure and the temperature on the

I. Galan (✉) · C. Andrade
Research Centre for Safety and Durability of Structures
and Materials, CISDEM-CSIC, Serrano Galvache 4,
28033 Madrid, Spain
e-mail: isabelgalan@ietcc.csic.es

F. P. Glasser
Department of Chemistry, University of Aberdeen,
Meston Walk, Aberdeen AB24 3UE, UK

calcium carbonate decomposition and to re-evaluate the parameters reported by Hyatt et al. [1]. It is also intended to provide experimental data that can serve to make the calculations for obtaining the kinetic parameters. Finally, the study should allow a better understanding of the factors controlling the shape of TG curves from carbonated cement paste samples.

Experimental

The material used is commercial CaCO_3 powder provided by Merck with purity of $>99.0\%$. The surface area of the powder was characterized by BET N_2 isotherms as $0.96 \pm 0.03 \text{ cm}^2/\text{mg}$. TG were performed in N_2 atmosphere at three different heating rates: 5, 10, and $20 \text{ }^\circ\text{C}/\text{min}$, and at constant heating rate $10 \text{ }^\circ\text{C}/\text{min}$, in three different atmospheres: N_2 and mixed nitrogen– CO_2 atmospheres with 20% CO_2 and 75% CO_2 . To get the different CO_2 concentrations in the atmospheres, N_2 and CO_2 were mixed in the furnace using mass flow controllers equipped with piezoelectric valves. The equipment used was a NETZSCH STA 449F3 DTA/TGA.

TG isotherms were done using different temperatures and atmospheres. The apparatus has two temperature thermocouples, one at the furnace and the other at the sample, the difference between the two being a constant 28 to $30 \text{ }^\circ\text{C}$ over the relevant temperature range. The sample thermocouple was calibrated using a set of standards (Ga, In, Sn, Bi, Zn, and Al) with well-known phase transition temperatures and reported temperatures are probably accurate up to $\pm 0.5 \text{ }^\circ\text{C}$. In N_2 , the temperatures of the isotherms (measured at the sample) were 641, 646, 671, 697, 721, 746, 770, 795, and $871 \text{ }^\circ\text{C}$. In the 20% CO_2 atmosphere, the temperatures used were 896, 922, 946, and $971 \text{ }^\circ\text{C}$; and finally, in the 75% CO_2 atmosphere, 911, 922, 947 and $972 \text{ }^\circ\text{C}$ were chosen. In all the cases, the samples were heated to the isotherm temperature at $20 \text{ }^\circ\text{C}/\text{min}$: no significant decomposition occurred during this initial heating.

100 mg of sample were used for both dynamic and isothermal experiments. The gas flow rate of $80 \text{ ml}/\text{min}$ was used in all the cases.

Results and discussion

Heating rate

Figure 1 shows the calcium carbonate decomposition in N_2 at three different heating rates: the left graph uses the x -axis for the temperature, and the right graph for time. Modifying the heating rate leads to a shift in the temperature range where the calcium carbonate decomposition takes place. Higher rates correspond to broader temperature decomposition ranges, namely, when increasing the rate, the decomposition is accelerated in terms of time and delayed in terms of temperature.

CO_2 concentration

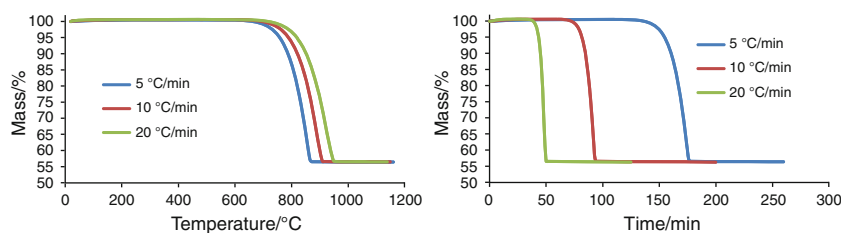
Increasing the CO_2 concentration in the atmosphere, namely the CO_2 partial pressure, displaces the equilibrium reaction toward calcium carbonate, making the decomposition shift to higher temperature. At a constant heating rate, higher CO_2 partial pressure leads to an increase in the onset temperature of the CaCO_3 decomposition (Fig. 2). In this case, changing the x -axis from temperature to time does not change the shape of the decomposition curve: the higher the CO_2 concentration in the atmosphere, the longer the time is required to complete the decomposition. The shape of the curve also approaches more closely to the ideal stepwise shape as the CO_2 partial pressure is increased.

Isotherms

As shown in Figs. 3, 4, 5, increasing the temperature of the isothermal decomposition leads to a shorter decomposition duration, namely, as an endothermic reaction, the CaCO_3 decomposition is favored when the temperature is increased. In N_2 (Fig. 3) at $871 \text{ }^\circ\text{C}$, CaCO_3 needs about 1 h to complete decomposition corresponding to a mass loss of $\sim 44\%$, while at $641 \text{ }^\circ\text{C}$ decomposition takes $\sim 24 \text{ h}$.

With the 20% CO_2 atmosphere (Fig. 4) at 971, 946, and $922 \text{ }^\circ\text{C}$, decomposition occurs within 2 h, while at $896 \text{ }^\circ\text{C}$, it takes more than 2 days. With the 75% CO_2 atmosphere (Fig. 5), the great increase in the decomposition time by lowering the temperature just 11 degrees is apparent, taking 4 h at $922 \text{ }^\circ\text{C}$ and 25 h at $911 \text{ }^\circ\text{C}$.

Fig. 1 CaCO_3 decomposition: heating rate comparison as a function of temperature and time



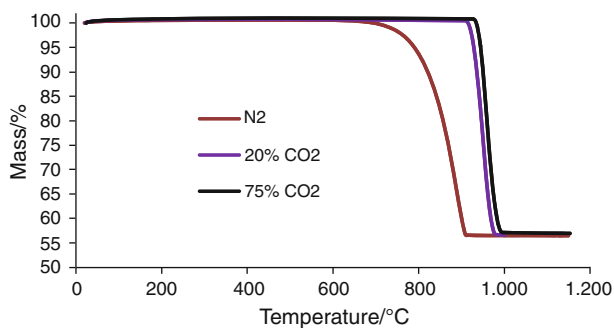


Fig. 2 TG curves from CaCO₃ decomposition as a function of partial pressure of carbon dioxide

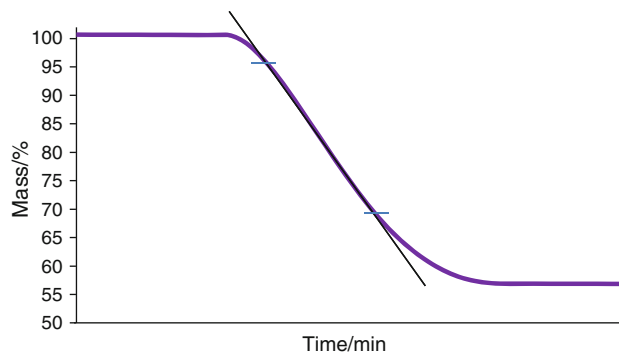


Fig. 6 Decomposition rate calculation: slope of linear part of the isothermal decomposition

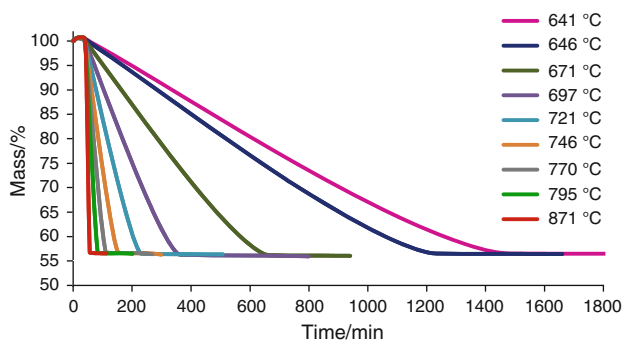


Fig. 3 Isothermal CaCO₃ decomposition in N₂

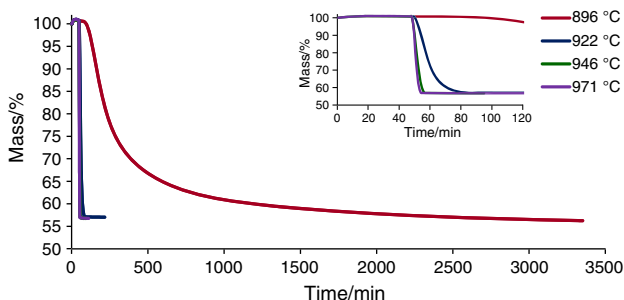


Fig. 4 Isothermal CaCO₃ decomposition in 20% CO₂ atmosphere

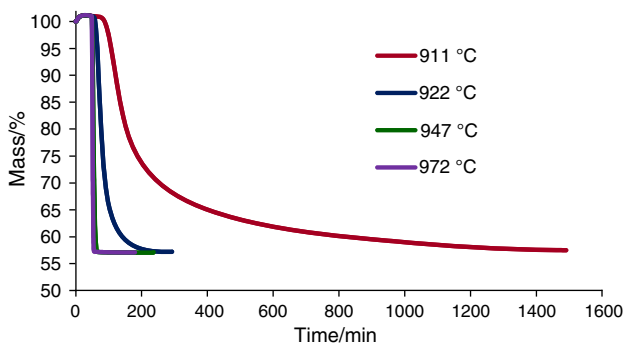


Fig. 5 Isothermal CaCO₃ decomposition in 75% CO₂ atmosphere

The first few minutes, during which no weight loss is recorded, correspond in most cases to the time taken for the samples to reach the isothermal temperature. However, in

the 896 °C and 20% CO₂ curve, as well as in the 911 and 922 °C in 75% CO₂ dataset, there is also a certain period where the final temperature will have been reached during which no weight loss takes place. These experiments, performed at the lowest temperatures, give information about the mechanism by which CaCO₃ decomposes in CO₂ atmospheres: the time interval represents at least in part an initial induction period before CaCO₃ begins to lose weight. The existence of an induction period was not, however, observed in analysis with pure N₂.

Decomposition rate

For calculating the decomposition rate, the slope of the linear part of the isothermal decomposition (% mass loss vs. time) was considered (Fig. 6). Dividing the decomposition rate by the BET area enables the rate to be expressed as mass loss per unit of time and sample surface area (mg/min cm²).

The calculated decomposition rates (*R*) at the temperatures considered in N₂ and in 20 and 75% CO₂ atmospheres are shown in Figs. 7, and 8, respectively. The *R* data can be fitted to an exponential function

$$R(T) = a \cdot \exp(T/\tau) - b \tag{1}$$

where *a*, *b*, and τ are positive constants that depend on the CO₂ partial pressure. The fitted curves and the corresponding equation are also shown in Figs. 7 and 8.

Using the equations obtained for *R*(*T*) for the different CO₂ concentrations, the values of *R* as a function of the CO₂ partial pressure can be obtained at different temperatures (Fig. 9).

Hyatt expression for the decomposition rate

The two main hypotheses of Hyatt et al. [1] are that (1) the decomposition reaction initiates at the surface of the calcite grains, and (2) the CaO initially formed is in an unstable structural state between the original rhombohedral CaCO₃

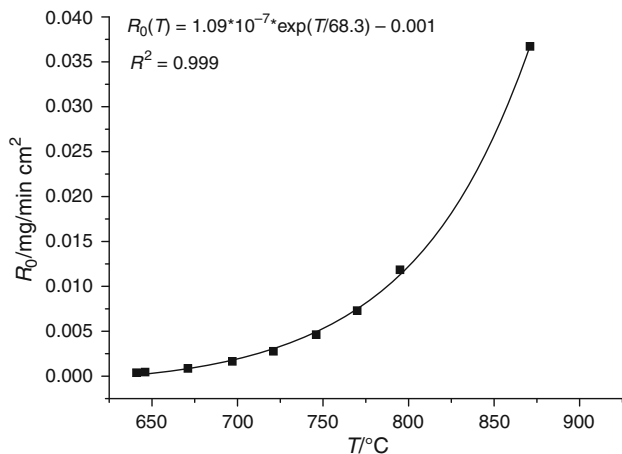


Fig. 7 Fitting of decomposition rate and evaluation of R: data for N₂ atmosphere

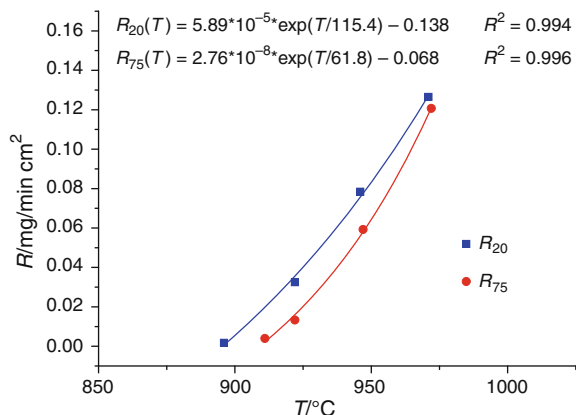


Fig. 8 Fitting of decomposition rate and evaluation of R: data for 20 and 75% CO₂ atmospheres

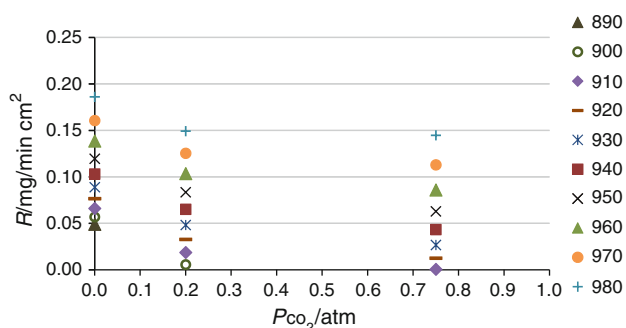


Fig. 9 R versus P_{CO₂}. Data obtained from equations in Figs. 7 and 8: experimental data

and the final well-crystallized cubic CaO. Based on these assumptions and on the equilibrium constants, the expression proposed for the decomposition rate in relation to decomposition rate in pure N₂ atmosphere is as follows:

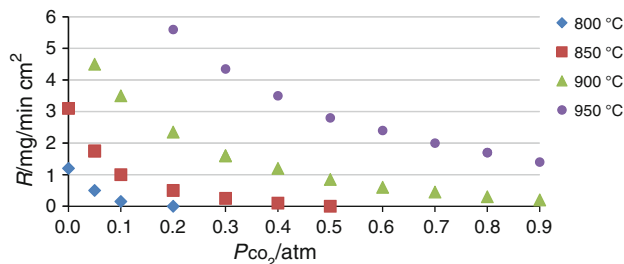


Fig. 10 R versus P_{CO₂}. Data are taken from [1]. Calcite crystals 0.1 × 1 × 1.5 cm

$$R = \frac{1 - P_{CO_2} / P_{CO_2}^0}{B \cdot P_{CO_2} + 1/R_0} \tag{2}$$

where P_{CO₂}⁰ is the equilibrium CO₂ partial pressure, P_{CO₂} is the CO₂ partial pressure, R₀ is the decomposition rate in N₂, and B is temperature dependant.

Figure 10 shows values drawn from Hyatt fittings of R versus P_{CO₂}.

P_{CO₂}⁰ is a function of the temperature only: the values for our calculations were taken from Hyatt (Fig. 11). The values of R₀(T) and R(T) have been calculated for 0, 20, and 75% CO₂ atmospheres (Figs. 7, 8). The values of P_{CO₂} are known from the concentration of CO₂ in the furnace. It should be noted that the CO₂ evolving from the CaCO₃ decomposition changes slightly the partial pressure of the surroundings of the sample, although there is a continuous flow of gas sweeping away the evolved gas. This means isobaric conditions are not reached all the time in the vicinity of the sample: P_{CO₂} is an average P_{CO₂}. Although total pressure is 1 bar, constant partial pressure of carbon dioxide is not achieved; moreover, despite other factors being equal, the difference lessens as P_{CO₂} increases.

For the calculation of B(T), the obtained values of R versus P_{CO₂} from the experimental data (Fig. 9) were fitted to Hyatt’s equation, fixing P_{CO₂}⁰ (Fig. 11) and R₀ (experimental). The values of B obtained from this calculation as well as the fitting to an exponential function

$$B(T) = -2.74 + 6.15 \cdot 10^{32} \cdot \exp(-T/12.92) \tag{3}$$

are shown in Fig. 12. This expression is valid for every partial pressure of CO₂ because B is dependent on temperature but not on P_{CO₂}.

The results obtained allow us to express the decomposition rate as a function of the CO₂ partial pressure and temperature, namely, although the materials studied are different (mainly due to differences in surface area), the Hyatt equation is assumed to apply.

However, the values obtained for powder differ considerably from those obtained from large crystals: both R₀ and R are much smaller for powder than for large crystals.

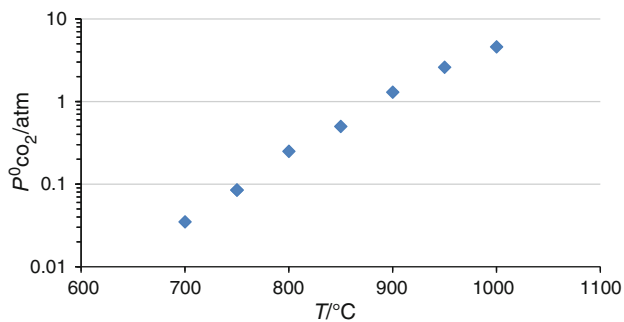


Fig. 11 $P^0_{\text{CO}_2}$ versus T . Values after Hyatt et al. [1]

This can be clearly seen comparing Figs. 9 and 10. For example, at 950 °C $R_0(\text{powder})$ is $0.12 \text{ mg min}^{-1} \text{ cm}^{-2}$ (Fig. 9) while $R_0(\text{crystal})$ is $\sim 14 \text{ mg min}^{-1} \text{ cm}^{-2}$ (Fig. 10). Also at 950 °C in 20% CO_2 atmosphere, the values for powder and crystal are 0.08 and 5.6, respectively. Regarding the differences between B values obtained for the two types of materials, they are much higher for powder than for large crystals. As an example, and deducing Hyatt B values from Fig. 10 data, at 950 °C $B(\text{crystal})$ is $0.4 \text{ min cm}^2 \text{ mg}^{-1} \text{ atm}^{-1}$ while $B(\text{powder})$ is $5.9 \text{ min cm}^2 \text{ mg}^{-1} \text{ atm}^{-1}$ (Fig. 12).

The decomposition mechanisms seem similar, but the parameters proposed by Hyatt cannot be applied to powder and vice versa. One of the reasons for this may be related to the changing CO_2 pressure around the grains as CO_2 is evolved in the course of decomposition. Depending on the furnace design and on the grain size of the particles, the composition of the atmosphere gas close to the grains may differ from the input gas composition. The most extreme assumption, where the atmosphere in the vicinity of a decomposing particle becomes 100% CO_2 , irrespective of the input gas composition, may give a partial explanation for the changing numerical values of B and R . As was

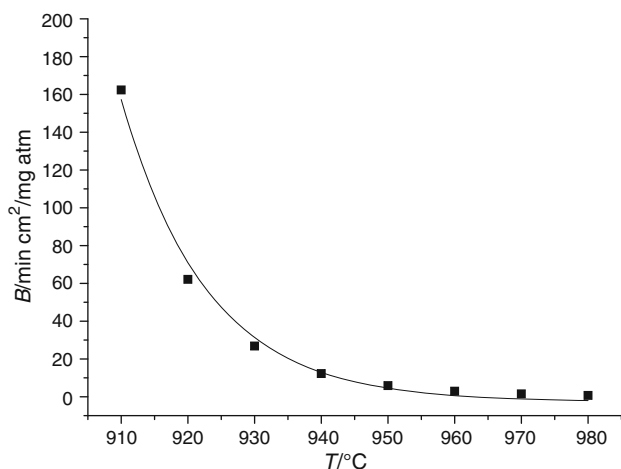


Fig. 12 Calculated B values from experimental data

shown before, the higher the CO_2 concentration, the slower the decomposition would be. In the case of powder, a greater surface area is decomposing at the same time compared to large crystals. This would imply a greater but local increase of CO_2 partial pressure in the powder decomposition which in turn would delay the reaction and lower the decomposition rate.

As there is no easy or certain way to deconvolute all the variables affecting the process, the use of isobaric conditions, i.e., the constant pressure of the volatile phase, in this instance, CO_2 , should be a benchmark for continuing this study in the future. Further research should include decompositions in 100% CO_2 atmospheres where the differences between different calcites cannot be due to extrinsic causes, but to intrinsic chemical differences.

Regarding the influence of defects on the results, it is considered that because of the relatively long time required to reach a steady temperature, point defects will be close to equilibrium. This means point defects in excess of equilibrium will anneal out in the course of heating. On the other hand, most particle size effects are unlikely to anneal out because sintering is slow. These effects manifest themselves as strains and could influence significantly decomposition. It seems plausible that sintering may take place during heating of nanoparticles. Future study should include the preparation and characterization of calcite nanoparticles to determine if the high surface area persists during heating and is sufficient to influence the subsequent thermal characteristics of the material.

Another point to be addressed in future studies is the question of “amorphous” material and its probable disappearance because of crystallization during annealing in CO_2 atmospheres at temperatures between 700 and 850 °C. By taking a sample close to decomposition, cooling, and measuring the BET surface, the roles of sintering and reduction of surface can be evaluated. In N_2 or CO_2 -poor atmosphere, where some decomposition occurs at low temperature, the persistence of amorphous material might still be observed.

Conclusions

The results obtained allow for a better understanding of the origin of TG data obtained from carbonated cement paste samples.

Definite indications were obtained regarding the existence of an induction period before CaCO_3 decomposition. These indications were the strongest in low-temperature decompositions in CO_2 -containing atmospheres.

The decomposition rate of CaCO_3 can be expressed as a function of the temperature and the CO_2 partial pressure: $R(T, P_{\text{CO}_2})$, substituting the expressions for $R_0(T)$, $P^0_{\text{CO}_2}(T)$ and $B(T)$.

Although the materials studied are different—mainly the surface area—Hyatt et al. equation applies also for calcium carbonate powder decomposition.

The parameters obtained for powder differ considerably to the ones obtained in large crystals: B values are much higher for powder than for large crystals, and both R_0 and R are much smaller for powder than for large crystals. Atmospheres rich in CO_2 give weight losses which are sharper and correspond closely to the ideal step profile. Consequently, measurement of evolved CO_2 , and hence calcite content, is less subject to interference from other thermal events. Controlled atmospheres rich in CO_2 allow for a better calculation of the kinetic parameters.

By using atmospheres at constant P_{CO_2} , the reversibility of reaction can also be established. The closer the reaction achieved under equilibrium conditions, the greater the justification for applying equilibrium thermodynamics.

References

- Hyatt EP, Cutler IB, Wadsworth ME. Calcium carbonate decomposition in carbon dioxide atmosphere. *J Am Ceram Soc.* 1958;41:70–4.
- Taylor HFW. Studies on the chemistry and microstructure of cement pastes. *Br Ceram Soc.* 1984;35:65–82.
- Parrott LJ, Killoh DC. Carbonation in a 36 year old, in situ concrete. *Cem Concr Res.* 1989;19:649–56.
- Rahman AA, Glasser FP. Comparative studies of the carbonation of hydrated cements. *Adv Cem Res.* 1989;2:49–54.
- Papadakis VG, Vayenas CG, Fardis MN. Experimental investigation and mathematical modeling of the concrete carbonation problem. *Chem Eng Sci.* 1991;46:1333–8.
- Parrott LJ. Carbonation, moisture and empty pores. *Adv Cem Res.* 1991;4:111–8.
- Thiery M, Villain G, Dangla P, Platret G. Investigation of the carbonation front shape on cementitious materials: effects of the chemical kinetics. *Cem Concr Res.* 2007;37:1047–58.
- Villain G, Thiery M, Platret G. Measurement methods of carbonation profiles in concrete: thermogravimetry, chemical analysis and gammadensimetry. *Cem Concr Res.* 2007;37:1182–92.
- Galan I, Andrade C, Mora P, Sanjuan MA. Sequestration of CO_2 by concrete carbonation. *Environ Sci Technol.* 2010;44:3181–6.
- Gallagher PK, Johnson DW Jr. The effects of sample size and heating rate on the kinetics of the thermal decomposition of CaCO_3 . *Thermochim Acta.* 1973;6:67–83.
- Zsakó J, Arz HE. Kinetic analysis of thermogravimetric data-VII. Thermal decomposition of calcium carbonate. *J Therm Anal.* 1974;6:651–6.
- Caldwell KM, Gallagher PK, Johnson DW Jr. Effect of thermal transport mechanisms on the thermal decomposition of CaCO_3 . *Thermochim Acta.* 1977;18:15–9.
- Criado JM, Morales J, Rives V. Computer kinetic analysis of simultaneously obtained TG and DTG curves. *J Therm Anal.* 1978;14:221–8.
- Criado JM, Rouquerol F, Rouquerol J. Thermal decomposition reactions in solids: comparison of the constant decomposition rate thermal analysis with the conventional TG method. *Thermochim Acta.* 1980;38:109–15.
- Darroudl T, Searcy AW. Effect of CO_2 pressure on the rate of decomposition of calcite. *J Phys Chem.* 1981;85:3971–4.
- Ray HS. The kinetic compensation effect in the decomposition of calcium carbonate. *J. Therm Anal.* 1982;24:35–41.
- Maciejewski M, Oswald HR. Morphological observations on the thermal decomposition of calcium carbonate. *Thermochim Acta.* 1985;85:39–42.
- Criado JM, Ortega A. A study of the influence of particle size on the thermal decomposition of CaCO_3 by means of constant rate thermal analysis. *Thermochim Acta.* 1992;195:163–7.
- Mulokozi AM, Lugwisha E. New aspects of the decomposition kinetics of calcite. Part 1. Isothermal decomposition. *Thermochim Acta.* 1992;194:375–83.
- Palandri A, Gilot P, Prado G. A kinetic study of the decarbonation of CaCO_3 . *J Anal Appl Pyrolysis.* 1993;27:119–30.
- Alcalá MD, Criado JM, Gotor FJ, Ortega A, Maqueda LAP, Real C. Development of a new thermogravimetric system for performing constant rate thermal analysis (CRTA) under controlled atmosphere at pressures ranging from vacuum to 1 bar. *Thermochim Acta.* 1994;240:167–73.
- Wang Y, Thomson WJ. The effect of sample preparation on the thermal decomposition of CaCO_3 . *Thermochim Acta.* 1995;255:383–90.
- Wei H, Luo Y. A study on the kinetics of thermal decomposition of CaCO_3 . *J Therm Anal.* 1995;45:303–10.
- Xiao X, Sichen DU, Sohn HY, Seetharaman S. Determination of kinetic parameters using differential thermal analysis-application to the decomposition of CaCO_3 . *Metal Mater Trans B.* 1997;28:1157–64.
- L'Vov BV, Polzik LK, Ugolkov VL. Decomposition kinetics of calcite: a new approach to the old problem. *Thermochim Acta.* 2002;390:5–19.
- Ren YL, Wang M, Li RS. The influence of morphology of ultra-fine calcite particles on decomposition kinetics. *J Therm Anal Calorim.* 2008;91:867–71.
- Anbalagan G, Rajakumar PR, Gunasekaran S. Non-isothermal decomposition of Indian limestone of marine origin. *J Therm Anal Calorim.* 2009;97:917–21.
- Odak B, Kosor T. Quick method for determination of equilibrium temperature of calcium carbonate dissociation. *J Therm Anal. Calorim.* doi:10.1007/s10973-011-2032-5.